Phonons in Si-Ge systems: An *ab initio* interatomic-force-constant approach

Stefano de Gironcoli
Institut Romand de Recherche Numérique en Physique des Matériaux (IRRMA), PHB-Ecublens, CH-1015 Lausanne, Switzerland
(Received 13 January 1992)

The vibrational properties of Si-Ge systems are studied theoretically with *ab initio* techniques. Full dispersion relations for pure silicon and germanium crystals under several (homogeneous and epitaxial) strain conditions are obtained from *interatomic* force constants (IFC's). High-symmetry vibrations for a few short-period ordered superlattices (SL's) are studied from first principles as well. In order to study conveniently more complicated systems, such as partially disordered SL's or homogeneous Si_xGe_{1-x} alloys, *higher-order* IFC's have been obtained that account for the first-order change in the IFC's of a reference system because of chemical disorder *and* lattice relaxation. With our scheme we can easily handle quite large supercells while keeping the same accuracy as a complete first-principles calculation, which we demonstrate for the homogeneous alloy.

I. INTRODUCTION

It is by now possible to grow atomically controlled semiconductor heterostructures, and by far the most studied among epitaxially grown systems are GaAs/AlAs and Si/Ge superlattices (SL's) and alloys for their possible technological applications. Much effort is presently devoted to understanding their vibrational properties both from experimental[1–5] and theoretical[6–9] points of view. Besides the fundamental interest in the properties of these peculiar materials, this effort is due to the possibility of characterizing these materials with use of Raman spectroscopy.

While many general aspects of phonons in a SL can already be understood within simple models, a more quantitative description and a proper account for strain and disorder effects is certainly desirable and still lacking. The limited predicting power of empirical models can be traced back to the absence of experimental information on which they strongly rely. In the case of GaAlAs systems, for instance, almost nothing is experimentally known on the AlAs bulk dispersion, and in the case of Si-Ge systems very little can be said about the effect of strain and atomic relaxation.

From the theoretical point of view, *ab initio* methods based on density-functional theory[10] in the local-density approximation[11] offer a unique opportunity to overcome the lack of experimental information. Over the last decade *ab initio* methods have proved to be very accurate and predictive tools for studying structural and vibrational properties of real materials. Recently, efficient linear-response techniques[12,13] have been introduced which allow us to obtain accurate phonon dispersions in the entire Brillouin zone (BZ) for systems of moderate complexity (such as elemental and III-V semiconductors) from the computation of *interatomic* forces constants (IFC's).

Direct first-principles calculations of phonons in SL's are also possible within the same approach but are still computationally very demanding and are thus limited to short-period perfectly ordered SL's.[14] In the special case of GaAlAs systems (SL's and alloys), strain is absent and the IFC's for the pure materials are very similar. Therefore it is possible to describe accurately the pure materials and all their compounds with a unique set of interatomic force constants obtained for the average crystal, taking into account only the difference in atomic mass between cations (mass approximation).[15] This approach has allowed us to study realistically the vibrational properties of homogeneous $Ga_xAl_{1-x}As$ alloy[16] and the role played by disorder at the interfaces on the vibrational properties of their SL's.[17] Instead in Si-Ge and other mixed systems a simple mass approximation does not work very well[13] due to the presence of strain and corrections beyond it are necessary.

In this paper we further develop the IFC's approach in the case of Si-Ge systems introducing *higher-order* IFC's that take into account the effects of strain. In Sec. II we analyze the effect of strain on the dispersions of the pure materials. Both homogeneous (hydrostatic) and epitaxial strain conditions are considered and the limited validity of the mass approximation is examined. In Sec. III we discuss how higher-order IFC's can be obtained which account for the effect of chemical disorder and lattice relaxation fitting the IFC's computed *ab initio* for a number of different strained crystals and chemical configurations. The reliability of the results obtained in this scheme is then demonstrated in Sec. IV against the accurate calculations of Sec. II and by comparison with direct calculation for a few selected short-period superlattices. We also apply our scheme to the study of the homogeneous Si_xGe_{1-x} alloys. Section V contains concluding remarks.

II. *AB INITIO* CALCULATIONS OF PHONONS IN SI AND GE UNDER STRAIN

In Ref. 13 it has been shown how accurate phonon dispersions for semiconductors can be obtained from first principles using first-order perturbation theory (in the pseudopotential-plane-wave formalism of density-functional theory). Here we apply this scheme to the study of silicon and germanium under strain.

The atomic pseudopotentials for Si and Ge used in this work are the same as in Ref. 13 and reproduce accurately the structural properties of the pure materials as shown in Table I. In particular, the lattice mismatch between the two materials is correctly reproduced. This is essential if we want to account properly for the effect of atomic relaxation in their compounds. Elastic constants are calculated using plane waves up to a high-kinetic-energy cutoff (26 Ry), which is necessary to get converged results,[18] whereas all the phonon calculations are performed with a 16-Ry cutoff, which guarantees a convergence in the calculated frequencies of 3 cm^{-1} or better. Ten Chadi-Cohen special points[19] are used for the BZ integration in the diamond structure, and the equivalent sampling when other structures are considered.

We consider three kinds of strained situations corresponding to a possible choice of the three independent macroscopic distortions in the diamond lattice: (i) Si and Ge under homogeneous strain, (ii) Si and Ge epitaxially grown on (001) direction on different substrates, and (iii) the same for (111) growth direction. In each case IFC's have been generated following Ref. 13 by Fourier transforming the dynamical matrices computed on a fine grid in the BZ (corresponding in real space to a fcc supercell of linear dimension four times larger than the bulk unit cell). IFC's up to the ninth shell of neighbors are thus obtained. Inclusion of even larger shell IFC's would not affect the optical branches, while the agreement with experimental data would be marginally better in the acoustic ones.

In Fig. 1 we show the results for homogeneous strain. For both silicon and germanium the solid lines give the results for the crystal at equilibrium (zero pressure). Comparison with experimental data shows the reliability of

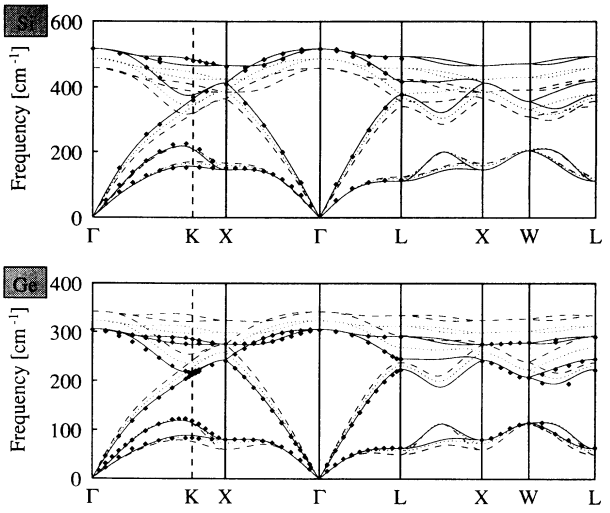

FIG. 1. Calculated phonon dispersions of elemental semiconductors Si and Ge under hydrostatic strain. Solid lines correspond to the unstrained situation, dashed lines correspond to silicon (germanium) at the germanium (silicon) lattice constant. The dotted lines are calculated at the virtual-crystal lattice constant in both cases. Experimental data (diamonds) are from Refs. 20 and 21.

ab initio calculations. The dashed lines correspond to Si (Ge) hydrostatically expanded (compressed) to the Ge (Si) lattice constant. The dotted lines correspond to the intermediate lattice constant of a $Si_{0.5}Ge_{0.5}$ alloy in both cases.

From the picture, the effect of homogeneous strain on dispersions appears essentially the same for the two materials. Under expansion (compression) the transverse-optical branches shift roughly rigidly toward lower (higher) values. The shifts at the high-symmetry points, Γ, X, and L, are -59, -80, and -69 cm^{-1} for silicon expanded to the germanium equilibrium lattice constant and $+38$, $+51$, and $+45$ cm^{-1} for germanium compressed to the silicon one. The transverse-acoustic branches behave in a more complex way, and

TABLE I. Structural parameters of Si and Ge. Lattice parameter are in atomic units, elastic constants in Mbar, the internal strain parameter (Ref. 24) ζ is dimensionless. Experimental data are given in parentheses.

	a	B	c_{11}	c_{12}	c_{44}	ζ
Si	10.20	0.93	1.59	0.60	0.77	0.53
	(10.26)[a]	(0.992)[b]	(1.675)[b]	(0.650)[b]	(0.801)[b]	(0.54)[c]
Ge	10.60	0.76	1.32	0.48	0.68	0.50
	(10.68)[a]	(0.768)[b]	(1.315)[b]	(0.494)[b]	(0.684)[b]	(0.54)[c]

[a] J. Donohue, *The Structures of the Elements* (Wiley, New York, 1974).

[b] H. J. McSkimin, J. Appl. Phys. **24**, 988 (1953); H. J. McSkimin and P. Andreatch, Jr. *ibid.* **35**, 3312 (1964).

[c] G. S. G. Cousins, L. Gerward, J. Staun Olsen, B. Selsmark, and B. J. Sheldon, J. Phys. C **20**, 29 (1987).

local minima are formed under compression at the symmetry points X and L. All shifts are in agreement with those that can be deduced from the experimental Grüneisen parameters[22] and are practically equal and opposite for the two materials when the difference in the atomic masses is taken into account. The longitudinal branches change differently along different directions. Along the Δ line they are well described by a rigid scaling of the frequencies in such a way that longitudinal and transverse modes are degenerate at Γ. This is an obvious effect of the degeneracy of optical and acoustic branches at X. As an effect of their different behavior, the crossing point along the Δ line of the longitudinal- and transverse-optical branches changes under strain.

We have then considered Si and Ge under the strain induced by growth on a substrate of different lattice parameter. In such epitaxial geometry the substrate fixes the in-plane lattice constant whereas the perpendicular one is left free to accomodate as much strain as is possible. The most studied substrate orientation is the (001) direction, and we have considered this one and the (111) direction, which give rise—together with the homogeneous strain considered above—to three independent strain patterns. We exhaust in this way the possible independent choices in a cubic material. For both (001) and (111) growth directions we have considered three in-plane lattice constants corresponding to silicon, germanium, and $Si_{0.5}Ge_{0.5}$ substrates. The structural parameters we have obtained by the requirement of zero stress in the growth direction are listed in Table II. In the case of (111) growth direction the atomic positions are not completely determined by the macroscopic lattice constants since the bonds formed in the (111) direction are not equivalent to the other bonds; there is in this case an internal degree of freedom that has to be determined requiring that no force acts on atoms. The atomic relaxation is described by the internal strain parameter, defined in Ref. 24, and the value is also given in Table II. In Figs. 2 and 3 we show the phonon dispersions obtained for (001) and (111) directions, respectively. The labeling of the symmetry points is kept as similar as possible to the one for the undistorted situation. In the (001) dispersions Z denotes the end point of the Δ line parallel to the growth direction, whereas in the (111) case L_z is the same for the Λ line. Again, solid lines correspond to the unstrained situation (the experimental data are not reported in this case), the dashed lines correspond to silicon (germanium) grown on a germanium (silicon) substrate, and the dotted lines correspond to the intermediate situation of a $Si_{0.5}Ge_{0.5}$ substrate.

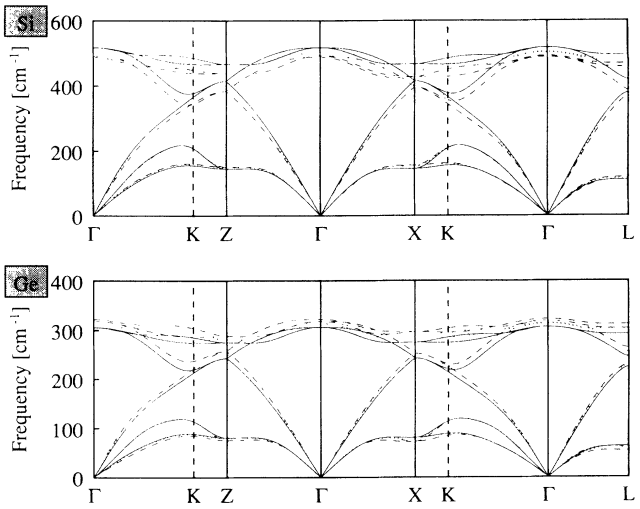

FIG. 2. Calculated phonon dispersions of elemental semiconductors Si and Ge grown on a (001) substrate. Solid lines correspond to the lattice-matched situation, dashed lines correspond to silicon (germanium) grown on a germanium (silicon) substrate. The dotted lines are calculated for a $Si_{0.5}Ge_{0.5}$ substrate in both cases.

The effect of strain can be analyzed in terms of the results for homogeneous strain. In fact the strain tensor appropriate to a given epitaxial geometry is a combination of a homogeneous and a traceless part. The main effect is due to the homogeneous part as described above, the effect of the traceless part being to remove the degeneracy along the Δ and Λ symmetry lines. For instance, for silicon grown on a Ge substrate in the (001) direction we have a -27-cm^{-1} average shift in the optical frequencies at Γ, which is consistent with the value obtained for the corresponding homogeneous strain alone in our calculation and from experimental Grüneisen[22] parameters (-24 cm^{-1}). The traceless part gives rise to

TABLE II. In-plane $a_\parallel$ and perpendicular $a_\perp$ lattice parameters (in a.u.) for Si and Ge grown in the (001) direction on different substrates as obtained by zero perpendicular stress condition. For (111) substrates the internal strain parameter (Ref. 24) ζ is also given.

		(001) substrate			(111) substrate		
		Si	$Si_{0.5}Ge_{0.5}$	Ge	Si	$Si_{0.5}Ge_{0.5}$	Ge
Si	$a_\parallel$	10.20	10.40	10.60	10.20	10.40	10.60
	$a_\perp/a_\parallel$	1.000	0.966	0.932	1.000	0.972	0.947
	ζ				0.53	0.51	0.48
Ge	$a_\parallel$	10.20	10.40	10.60	10.20	10.40	10.60
	$a_\perp/a_\parallel$	1.068	1.033	1.000	1.055	1.026	1.000
	ζ				0.55	0.52	0.50

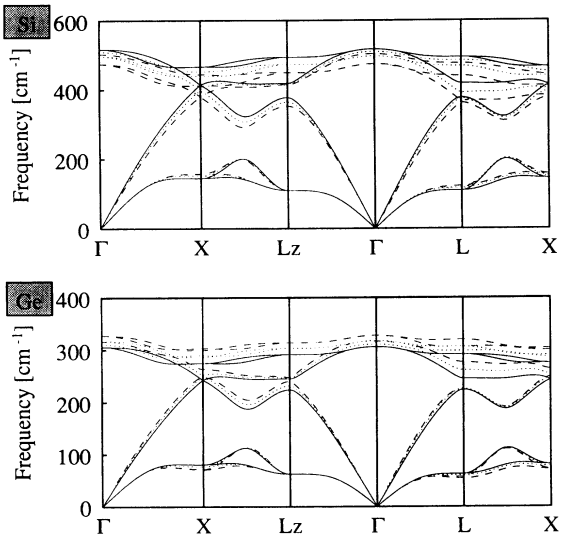

FIG. 3. Calculated phonon dispersions of elemental semiconductors Si and Ge grown on a (111) substrate. Same convention as in Fig. 2.

a longitudinal-optical–transverse-optical splitting of 3.7 cm^{-1}, which is roughly half of the experimental result[23] but in agreement with a previous *ab initio* calculation.[18] The disagreement between theory and experiment is in part due to the large strain considered for which contributions to the splitting nonlinear in the strain are important and is reduced by a factor of 2 in the less strained case of Si grown on $Si_{0.5}Ge_{0.5}$. A much larger splitting (as large as 29 cm^{-1} for Si grown on Ge) appears for the (111) growth direction, where the effects of the homogeneous and traceless part of the strain are of comparable size. Again the agreement with experiment is good for the average shift, and not as good (a 30% overestimation) for the splitting, partly due to nonlinearity. Similar results are obtained for germanium.

We discuss now the validity of mass approximation. As the effect of strain can be quite large, it is clear that it is not possible to find a unique set of IFC's that describe all situations. Different strain conditions require different sets of IFC's. The effect of a different chemical environment is less pronounced. If we limit our attention to pure materials at equilibrium, the use of the IFC's of the virtual crystal *at equilibrium* is not too bad (within 10–15 cm^{-1}) and gives very good results (3–5 cm^{-1}) if the dispersions obtained with the mass approximation are scaled with the ratio of the material and virtual-crystal plasma frequencies. The same happens if a distorted material is approximated with the IFC's of the virtual crystal under the *same* distortion. So, at least for Si-Ge systems where the chemical difference between the two atoms is quite small,[25] a unique set of IFC's can describe vibrational properties at fixed *strain condition*. Unfortunately this is of little help because in a real case we are interested in atomic configurations in which the chemical environment changes from site to site, and hence, due to the local atomic relaxation, the strain condition changes as well with the position. There is no simple satisfactory way to implement the nice scaling properties described above in the general case. We have then coped with this problem in a different way, as described in Sec. III.

III. HIGHER-ORDER INTERATOMIC FORCE CONSTANTS

In order to go beyond mass approximation we need to describe the effect on the dynamical matrices of the different chemical environment and atomic relaxation. Let us consider the total energy as a function of the atomic displacements $\{\mathbf{u_R}\}$ with respect to the diamond sites $\{\mathbf{R}\}$, and a set of Ising-like variables $\{\sigma_\mathbf{R}\}$, such that $\sigma_\mathbf{R} = +1$ if the atom sitting at the site $\mathbf{R}$ is Si and $\sigma_\mathbf{R} = -1$ if it is Ge. The vibrational force constants for a given atomic configuration—i.e., for a given distribution of $\{\sigma_\mathbf{R}\}$—are defined as the second derivatives of the total energy with respect to atomic displacements, computed at the equilibrium positions

$$C(\mathbf{R},\mathbf{R}';\{\sigma_\mathbf{R}\}) = \frac{\partial^2\mathcal{E}(\{\mathbf{u_{R_0}}\},\{\sigma_\mathbf{R}\})}{\partial\mathbf{u_R}\partial\mathbf{u_{R'}}}, \tag{1}$$

where $\{\mathbf{u_{R_0}}\}$ are such that

$$\frac{\partial\mathcal{E}(\{\mathbf{u_{R_0}}\},\{\sigma_\mathbf{R}\})}{\partial\mathbf{u_R}} = 0. \tag{2}$$

In the pseudopotential approach it is possible to consider the $\{\sigma_\mathbf{R}\}$ as continuous variables rather than just ±1, assuming that for a given σ the corresponding atom is represented by the pseudopotential $V_\sigma(\mathbf{r}) = [(1+\sigma)/2]V_{\mathrm{Si}}(\mathbf{r}) + [(1-\sigma)/2]V_{\mathrm{Ge}}(\mathbf{r})$, which reduces to the previous definition at the end points and interpolates linearly in between.

We can then expand the total energy with respect to all variables, $\{\mathbf{u_R}\}$ and $\{\sigma_\mathbf{R}\}$:

$$\begin{aligned}\mathcal{E}(\{\mathbf{u_R}\},\{\sigma_\mathbf{R}\}) = \mathcal{E}_0 &+ \sum_\mathbf{R}\frac{\partial\mathcal{E}}{\partial\mathbf{u_R}}\mathbf{u_R} + \frac{\partial\mathcal{E}}{\partial\sigma_\mathbf{R}}\sigma_\mathbf{R} \\ &+\tfrac{1}{2}\sum_{\mathbf{R},\mathbf{R}'}\left(\frac{\partial^2\mathcal{E}}{\partial\sigma_\mathbf{R}\partial\sigma_{\mathbf{R}'}}\sigma_\mathbf{R}\sigma_{\mathbf{R}'}\right. \\ &\qquad +2\frac{\partial^2\mathcal{E}}{\partial\sigma_\mathbf{R}\partial\mathbf{u_{R'}}}\sigma_\mathbf{R}\mathbf{u_{R'}} \\ &\qquad \left.+\frac{\partial^2\mathcal{E}}{\partial\mathbf{u_R}\partial\mathbf{u_{R'}}}\mathbf{u_R}\mathbf{u_{R'}}\right)+\cdots,\end{aligned} \tag{3}$$

or equivalently

$$\begin{aligned}\mathcal{E}(\{\mathbf{u_R}\},\{\sigma_\mathbf{R}\}) = \mathcal{E}_0 &+ \sum_\mathbf{R} K\sigma_\mathbf{R} \\ &+\tfrac{1}{2}\sum_{\mathbf{R},\mathbf{R}'}[J(\mathbf{R}-\mathbf{R}')\sigma_\mathbf{R}\sigma_{\mathbf{R}'} \\ &\qquad +2\mathbf{F}(\mathbf{R}-\mathbf{R}')\sigma_\mathbf{R}\mathbf{u_{R'}} \\ &\qquad +\mathbf{\Phi}(\mathbf{R}-\mathbf{R}')\mathbf{u_R}\mathbf{u_{R'}}]+\cdots,\end{aligned} \tag{4}$$

where the ellipses represent higher-order terms, and where all the derivatives are taken at the equilibrium positions $\{\mathbf{u_R}=0\}$ of the virtual crystal $\{\sigma_\mathbf{R}=0\}$. By truncating this expansion at a given level one has a controlled approximation to the energetics of the system and

can study its vibrational properties as well as its thermodynamics within this approximation. The energetics of Si-Ge systems is well described[25] by terms up to the second order that can be computed with our efficient linear-response techniques. For the vibrational properties this is not the case. In fact, truncating the energy expansion at the second-order term yields the virtual-crystal force constants for all configurations, i.e., we recover the mass approximation. This happens to be an excellent approximation for GaAlAs systems[16,17] but not for the SiGe system as discussed before.

The natural way to go beyond mass approximation is then to retain also the following order in the Taylor expansion of Eq. (4), i.e., the third-order derivatives of the total energy

$$\begin{aligned}
\frac{\partial^3 \mathcal{E}}{\partial \mathbf{u}_{\mathbf{R}} \partial \mathbf{u}_{\mathbf{R}'} \partial \mathbf{u}_{\mathbf{R}''}} &= \mathbf{\Phi}^{(1)}(\mathbf{R}-\mathbf{R}'', \mathbf{R}'-\mathbf{R}''), \\
\frac{\partial^3 \mathcal{E}}{\partial \mathbf{u}_{\mathbf{R}} \partial \mathbf{u}_{\mathbf{R}'} \partial \sigma_{\mathbf{R}''}} &= \mathbf{F}^{(1)}(\mathbf{R}-\mathbf{R}'', \mathbf{R}'-\mathbf{R}''), \\
\frac{\partial^3 \mathcal{E}}{\partial \mathbf{u}_{\mathbf{R}} \partial \sigma_{\mathbf{R}'} \partial \sigma_{\mathbf{R}''}} &= \mathbf{J}^{(1)}(\mathbf{R}-\mathbf{R}'', \mathbf{R}'-\mathbf{R}''), \\
\frac{\partial^3 \mathcal{E}}{\partial \sigma_{\mathbf{R}} \partial \sigma_{\mathbf{R}'} \partial \sigma_{\mathbf{R}''}} &= L(\mathbf{R}-\mathbf{R}'', \mathbf{R}'-\mathbf{R}'').
\end{aligned} \tag{5}$$

The IFC's for a given configuration are then given by

$$\begin{aligned}
\mathbf{\Phi}_{\{\mathbf{u}_{\mathbf{R}}, \sigma_{\mathbf{R}}\}}(\mathbf{R}, \mathbf{R}') = \mathbf{\Phi}(\mathbf{R}-\mathbf{R}') &+ \sum_{\mathbf{R}''} \mathbf{\Phi}^{(1)}(\mathbf{R}-\mathbf{R}'', \mathbf{R}'-\mathbf{R}'')\mathbf{u}_{\mathbf{R}''} \\
&+ \mathbf{F}^{(1)}(\mathbf{R}-\mathbf{R}'', \mathbf{R}'-\mathbf{R}'')\sigma_{\mathbf{R}''}.
\end{aligned} \tag{6}$$

All the third-order derivatives could in principle be obtained directly from a linear-response calculation for the virtual crystal,[26] but it is easier to extract these higher-order IFC's (HIFC's) from fits of Eq. (6) for a number of independent configurations. In order to fit $\mathbf{\Phi}^{(1)}$, the IFC's of virtual crystal under three independent distortions—homogeneous, traceless distortion in the (001) and (111) directions—have been considered. As for $\mathbf{F}^{(1)}$'s, we have fitted the IFC's of Si, Ge, and zinc-blende SiGe with atoms frozen at the atomic positions of the virtual crystal. Additional general constraints have been used to reduce the number of independent parameters. These constraint are of three kinds: (i) we require permutation symmetry of the order of the derivatives in Eq. (5) to be satisfied; (ii) we impose the acoustic sum rule (ASR) for a generic configuration, which implies

$$\sum_{\mathbf{R}} \mathbf{\Phi}^{(1)}(\mathbf{R}-\mathbf{R}'', \mathbf{R}'-\mathbf{R}'') = 0, \tag{7}$$

$$\sum_{\mathbf{R}} \mathbf{F}^{(1)}(\mathbf{R}-\mathbf{R}'', \mathbf{R}'-\mathbf{R}'') = 0, \tag{8}$$

for all $\mathbf{R}'$ and $\mathbf{R}''$; (iii) we require that the first-order variations $\mathbf{\Phi}^{(1)}$ and $\mathbf{F}^{(1)}$ correctly describe the effect of rotations,

$$\begin{aligned}
\sum_{\mathbf{R}'} \sum_{\rho,\sigma} \mathbf{\Phi}^{(1)}{}_{\alpha\beta\sigma}(\mathbf{R}-\mathbf{R}'', \mathbf{R}'-\mathbf{R}'') e_{\gamma\sigma\rho}(\mathbf{R}'-\mathbf{R}'')_\rho \\
= \sum_{\sigma} e_{\gamma\alpha\sigma} \mathbf{\Phi}_{\sigma\beta}(\mathbf{R}-\mathbf{R}') + \sum_{\sigma} e_{\gamma\sigma\beta} \mathbf{\Phi}_{\alpha\sigma}(\mathbf{R}-\mathbf{R}'), \\
\sum_{\mathbf{R}''} \sum_{\sigma,\rho} \mathbf{F}^{(1)}{}_{\alpha\sigma}(\mathbf{R}-\mathbf{R}'', \mathbf{R}'-\mathbf{R}'') e_{\gamma\sigma\rho}(\mathbf{R}'-\mathbf{R}'')_\rho \\
= \sum_{\sigma} e_{\gamma\alpha\sigma} \mathbf{F}_{\sigma}(\mathbf{R}-\mathbf{R}'),
\end{aligned} \tag{9}$$

where $e_{\alpha\beta\gamma}$ is the Levi-Civita tensor.

Finally we require the effect of strain and chemical disorder to be only local and we allow $\mathbf{\Phi}^{(1)}$ and $\mathbf{F}^{(1)}$ to be nonvanishing only for those triplet of sites that contain at least one first-nearest-neighbor pair and at most second-nearest-neighbors ones. This restriction is probably not serious for $\mathbf{F}^{(1)}$ since the other quantities $\mathbf{F}$ and J that correspond to derivatives with respect to $\sigma_{\mathbf{R}}$ are very short ranged.[25] This approximation is less justified for $\mathbf{\Phi}^{(1)}$ since it is well known that in Si and Ge the IFC's are quite long ranged along the bond chains in the (110) planes[27] (which is an essential feature to explain the characteristic flatness of their acoustic branch). We do not expect the HIFC's we will obtain to give completely satisfactory results in this region.

All these constraints are imposed by least square minimization. The resulting HIFC's reproduce the *ab initio* results within 3–5 cm^{-1}, when used for the fitted structures. This is essentially the agreement between the *ab initio* calculation itself and the experimental results, when available. We note in passing that the experimental results for the strain-induced splitting in optical modes at Γ point[23] turn out to be somewhat better reproduced with the HIFC's than in the original *ab initio* calculations.

IV. TESTING HIGHER-ORDER INTERATOMIC FORCE CONSTANTS

To assess the reliability of the HIFC's it is obviously not sufficient to compare with the fitted structures but they have to be checked against calculation in structures other than the fitted ones. This is done in Table III and Fig. 4.

In Table III we compare the frequencies calculated *ab initio* and with the HIFC's for some high-symmetry points in Si and Ge under homogeneous strain. From this table we see that the HIFC's reproduce the *ab initio* results within a few cm^{-1}—sometimes worse, as expected, in the acoustic region—over a range of distortions which corresponds to frequency shifts of several tens of cm^{-1}. Analogous results are obtained for the other strain conditions considered in Sec. II and the general description of the phonon dispersion relations is quite satisfactory. A more stringent test of the soundness of HIFC's is given by the results for short-period SL's where the chemical environment is qualitatively different from the bulk case. We have considered some very short-period SL's matched to

TABLE III. Phonon frequencies calculated at high-symmetry points Γ, X, L, for Si and Ge under homogeneous strain. The considered lattice parameters are given in atomic units. In each case the first entry refers to the calculation with the higher-order IFC's, the second one (in parentheses) to the *ab initio* calculation.

	Silicon			Germanium		
	10.20	10.40	10.60	10.20	10.40	10.60
Γ_{LTO}	519 (517)	488 (487)	456 (458)	343 (342)	325 (321)	307 (303)
X_{TA}	136 (145)	152 (158)	166 (165)	60 (60)	74 (74)	85 (81)
X_{LOA}	414 (414)	391 (389)	367 (366)	273 (274)	260 (257)	245 (241)
X_{TO}	471 (466)	431 (425)	386 (386)	324 (324)	301 (296)	276 (273)
L_{TA}	103 (110)	114 (118)	123 (123)	49 (50)	58 (58)	65 (63)
L_{LA}	376 (378)	369 (368)	341 (342)	235 (237)	231 (230)	226 (223)
L_{TO}	497 (494)	462 (458)	424 (425)	334 (334)	314 (310)	293 (289)
L_{LO}	423 (419)	384 (379)	362 (358)	292 (293)	270 (266)	247 (243)

$Si_{0.5}Ge_{0.5}$. The phonon dispersions for $(Si)_2/(Ge)_2$ SL's grown in the (001) and (111) directions are shown in Fig. 4. In the (111) direction there are two unequivalent SL's according to the stacking of the layers:[28] RH1 if the (111) bonds are homopolars (Si-Si or Ge-Ge), RH2 if they are heteropolars (Si-Ge). In Fig. 4 the solid line is given by HIFC's whereas diamonds indicate the results of *ab initio* calculations for high-symmetry points. Also in this case the agreement is very good and hence we conclude that HIFC's yield a safe approximation for the vibrational properties of complex Si-Ge systems.

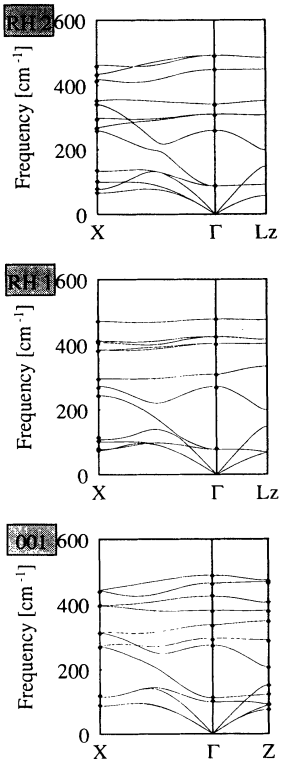

FIG. 4. Calculated phonon dispersions of short-period Si_2/Ge_2 (001) and (111) SL's. In the (111) direction two SL's are possible—RH1 and RH2—depending on the layer stacking. Solid lines are obtained with HIFC's, diamonds show the result of a direct *ab initio* calculation.

As a final test of our approach we consider the vibrational properties of homogeneous $Si_{1-x}Ge_x$ alloys. Their Raman spectra are known for a long time[29] to exhibit three strong peaks at $\sim$ 300, 400, and 500 cm^{-1}, corresponding to Ge-Ge, Si-Ge, and Si-Si bond vibrations, respectively. Recently a detailed investigation[30] of epitaxially grown and polycrystalline Si-Ge alloys has determined accurately the position of the main peaks and of additional weak structures in the frequency region between 400 and 500 cm^{-1}, corresponding to Si vibrations in chemically different local environments. We will calculate Raman spectra for free-standing $Si_{1-x}Ge_x$ alloys at the same composition as in Ref. 30.

We describe a disordered alloy with a supercell geometry in which Si and Ge atoms are randomly distributed according to the considered composition. This is consistent with the experimental picture of bulk $Si_{1-x}Ge_x$ as a model random alloy[31] and with previous theoretical finding[25,32,33] of no clustering or ordering in the bulk alloys at room temperature. The lattice parameter is assumed to vary with composition according to Vegard's law. Our simulation cell contains 512 atoms periodically repeated throughout the space. Dynamical matrix and forces on atoms are computed from HIFC's and atomic positions are relaxed iteratively until equilibrium is reached. Standard diagonalization of the dynamical matrix at equilibrium then yields phonon frequencies and displacement patterns for our sample. Raman spectra have been calculated as in Ref. 16, neglecting the difference in polarizability between Si and Ge and assuming the same symmetry-selection rules as in an undistorted diamond lattice. The Raman strength for incident and scattered lights polarized along ε^I and ε^F, respectively, is then given, up to a multiplicative constant, by

$$\sigma^{I,F}(\omega) \propto \sum_{\nu} \frac{\delta(\omega_\nu - \omega)}{\omega_\nu} \times \left| \sum_{\mathbf{R},\alpha,\beta,\gamma} s(\mathbf{R})\, |e_{\alpha\beta\gamma}|\, \varepsilon^I_\alpha \varepsilon^F_\beta u^\nu_\gamma(\mathbf{R}) \right|^2 , \quad (10)$$

where the sum runs over all supercell modes, $u^\nu_\gamma(\mathbf{R})$ is the displacement pattern for the νth one (with frequency ω_ν), and $s(\mathbf{R})$ is $+1$ and -1 in the two fcc sublattices of

TABLE IV. Peak frequencies, in cm^{-1}, for the main Raman-active modes in relaxed $Si_{1-x}Ge_x$ alloys as obtained in this work for three composition ($x = 0.28$, $x = 0.55$, $x = 0.77$). Experimental values from Ref. 30 are given for comparison.

x		Ge-Ge	Si-Ge	Si-Si	Weak peaks
0.28	Theory	295	409	501	440,451,(475)
	Expt.	287	404	502	247,430
0.55	Theory	297	410	485	430,449,(468)
	Expt.	290	407	482	428,446,(468)
0.77	Theory	300	405	466	425,443,460
	Expt.	295	404	468	425,443,459

the diamond structures. In the actual calculation the δ function is substituted with a 2-cm^{-1}-wide Lorentzian.

In Fig. 5 the resulting Raman spectra are shown for the three compositions considered ($x = 0.28$, $x = 0.55$, and $x = 0.77$). To reduce statistical errors three random configurations are considered for each composition and the spherically averaged Raman intensity, $\sigma = \frac{1}{3}(\sigma^{x,y} + \sigma^{x,z} + \sigma^{y,z})$, is computed. The agreement with the experimental results is quite satisfactory. Peak positions (arrows in the figure indicate their experimental values) and shapes are well reproduced by our calculation even for the weak structures in the 400–500-cm^{-1} region. The relative intensity for Ge-Ge, Si-Ge, and Si-Si peaks are not well reproduced due to the equal polarizability approximation. For a detailed comparison, in Table IV we report the peak positions as obtained in our calculation together with experimental data; the position of the shoulders near the main Si-Si peak is given in parentheses and is only tentatively assigned. The spectral features are very well reproduced for Si-Si and Si-Ge vibrations and are slightly worse for Ge-Ge ones, especially in the Si-rich sample. The almost perfect agreement with experiment for the weak structures is certainly somewhat fortuitous but nevertheless remarkable. A complete study of the vibrational properties of the $Si_{1-x}Ge_x$ alloy will be presented elsewhere.[34]

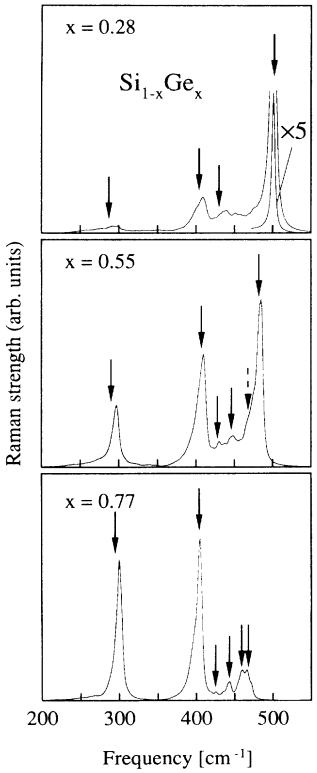

FIG. 5. Calculated Raman spectra of homogeneous $Si_{1-x}Ge_x$ alloys for three compositions ($x = 0.28$, $x = 0.55$, $x = 0.77$). The experimental positions (from Ref. 30) of the main Raman peaks and of the weak structures in the region between the main Si-Ge and Si-Si peaks are shown by arrows.

V. CONCLUSIONS

In this paper the vibrational properties of Si-Ge systems have been studied extensively. A set of higher-order interatomic force constants have been obtained from a density-functional calculation of interatomic force constants for different strain conditions and chemical environments. Using these force constants, complex systems—such as partially disordered SL's or homogeneous Si_xGe_{1-x} alloys—can be easily studied, keeping essentially the same accuracy of a complete first-principles calculation. We have applied our approach to the homogeneous Si_xGe_{1-x} alloys for a number of compositions, using large supercells to simulate disorder. The computed Raman spectra agree quite well with experimental data. This is a quantitatively accurate description of the vibrational properties of $Si_{1-x}Ge_x$ alloys that has been obtained theoretically. Our approach can be of great usefulness in the interpretation of experimental data for Si/Ge SL's, allowing us to account for the effect of interface roughness and atomic intermixing.

ACKNOWLEDGMENTS

We are grateful to S. Baroni, P. Giannozzi, and E. Molinari for many useful discussions and a critical reading of the manuscript. This work was supported in part by the Swiss National Science Foundation under Grant No. 20-5446.87.

[1]E. Friess, H. Brugger, K. Eberl, G. Krötz, and G. Abstreiter, Solid State Commun. **69**, 899 (1989); E. Friess, K. Eberl, U. Menczigar, and G. Abstreiter, *ibid.* **73**, 203 (1990); K. Eberl, W. Wegsheider, R. Schorer, and G. Abstreiter, Phys. Rev. B **43**, 5188 (1991).
[2]J. D. White, G. Fasol, R. A. Ghanbari, M. A. Gell, C. J. Gibbings, and C. G. Tuppen, Phys. Rev. B **43**, 1685 (1991).
[3]F. Cerdeira, M. I. Alonso, D. Niles, M. Garriga, M. Cardona, E. Kasper, and H. Kibbel, Phys. Rev. B **40**, 1361 (1989); M. I. Alonso, F. Cerdeira, D. Niles, M. Cardona, E. Kasper, and H. Kibbel, J. Appl. Phys. **66**, 5645 (1989).
[4]D. J. Lockwood, M. W. C. Dharma-wardana, G. C. Aers, and J.-M. Baribeau, Appl. Phys. Lett. **52**, 2040 (1988); M. W. C. Dharma-wardana, G. C. Aers, D. J. Lockwood, and J.-M. Baribeau, Phys. Rev. B **41**, 5319 (1990).
[5]J. C. Tsang, S. S. Iyer, and S. L. Delage, Appl. Phys. Lett. **51**, 1732 (1987); S. S. Iyer, J. C. Tsang, M. W. Copel, P. R. Pukite, and R. M. Tromp, *ibid.* **54**, 219 (1989).
[6]E. Molinari and A. Fasolino, Appl. Phys. Lett. **54**, 1220 (1989); A. Fasolino, E. Molinari, and J. C. Maan, Phys. Rev. B **39**, 3923 (1989); A. Qteish and E. Molinari, *ibid.* **42**, 7090 (1990).
[7]R. A. Ghambari, J. D. White, G. Fasol, C. J. Gibbings, and C. G. Tuppen, Phys. Rev. B **42**, 7033 (1990).
[8]M. I. Alonso, M. Cardona, and G. Kanellis, Solid State Commun. **69**, 479 (1989).
[9]P. Molinas-Mata and M. Cardona, Superlattices Microstruct. **10**, 39 (1991).
[10]P. Hohenberg and W. Kohn, Phys. Rev. **136**, B864 (1964).
[11]W. Kohn and L. J. Sham, Phys. Rev. **140**, A1133 (1965).
[12]S. Baroni, P. Giannozzi, and A. Testa, Phys. Rev. Lett. **58**, 1861 (1987).
[13]P. Giannozzi, S. de Gironcoli, P. Pavone, and S. Baroni, Phys. Rev. B **43**, 7231 (1991).
[14]S. Baroni, P. Giannozzi, and E. Molinari, Phys. Rev. B **41**, 3870 (1990).
[15]This mass approximation was introduced by Barker *et al.* for GaAs/AlAs superlattices in A. S. Barker Jr., J. L. Merz, and A. C. Gossard, Phys. Rev. B **17**, 3181 (1978).
[16]S. Baroni, S. de Gironcoli, and P. Giannozzi, Phys. Rev. Lett. **65**, 84 (1990).
[17]See, for instance, E. Molinari, S. Baroni, P. Giannozzi, and S. de Gironcoli in *Proceedings of the 20th International Conference on the Physics of Semiconductors*, edited by E. Anastassakis and J. D. Joannopulos (World Scientific, Singapore, 1990), p. 1427.
[18]O. H. Nielsen and R. M. Martin, Phys. Rev. B **32**, 3792 (1985).
[19]D. J. Chadi and M. L. Cohen, Phys. Rev. B **8**, 5747 (1973).
[20]G. Dolling, *Inelastic Scattering of Neutrons in Solids and Liquids* (IAEA, Vienna, 1963), Vol. II, p. 37; G. Nilsson and G. Nelin, Phys. Rev. B **6**, 3777 (1972).
[21]G. Nilsson and G. Nelin, Phys. Rev. B **3**, 364 (1971).
[22]B. A. Westein and G. J. Piermarini, Phys. Rev. B **12**, 1172 (1975); J. Buchenauer, F. Cerdeira, and M. Cardona, in *Proceedings of the 2nd International Conference of Light Scattering in Solids*, edited by M. Balkanski (Flammarion, Paris, 1971), p. 280.
[23]F. Cerdeira, C. J. Buchenauer, F. H. Pollak, and M. Cardona, Phys. Rev. B **5**, 580 (1972); M. Chandrasekhar, J. B. Renucci, and M. Cardona, *ibid.* **17**, 1623 (1978); E. Anastassakis, A. Cantarero, and M. Cardona, *ibid.* **41**, 7529 (1990).
[24]L. Kleinman, Phys. Rev. **128**, 2914 (1962).
[25]S. de Gironcoli, P. Giannozzi, and S. Baroni, Phys. Rev. Lett. **66**, 2116 (1991).
[26]X. Gonze and J.-P. Vigneron, Phys. Rev. B **39**, 13120 (1989).
[27]A. Fleszar and R. Resta, Phys. Rev. B **34**, 7140 (1986).
[28]A. Ourmazd and J. C. Bean, Phys. Rev. Lett. **55**, 765 (1985); F. K. LeGoues, V. P. Kesan, and S. S. Iyer, *ibid.* **64**, 40 (1990).
[29]J. B. Renucci, M. A. Renucci, and M. Cardona, Solid State Commun. **9**, 1651 (1971); W. J. Brya, Solid State Commun. **12**, 253 (1973); J. S. Lannin, Phys. Rev. B **16**, 1510 (1977).
[30]M. I. Alonso and K. Winer, Phys. Rev. B **39**, 10056 (1989).
[31]M. Hansen and K. Anderko, *Constitution of Binary Alloys*, 2nd ed. (McGraw Hill, New York, 1958), p. 774.
[32]A. Qteish and R. Resta, Phys. Rev. B **37**, 1308 (1988); **37**, 6983 (1988).
[33]J. E. Bernard and A. Zunger, Phys. Rev. B **44**, 1663 (1991).
[34]S. de Gironcoli and S. Baroni (unpublished).

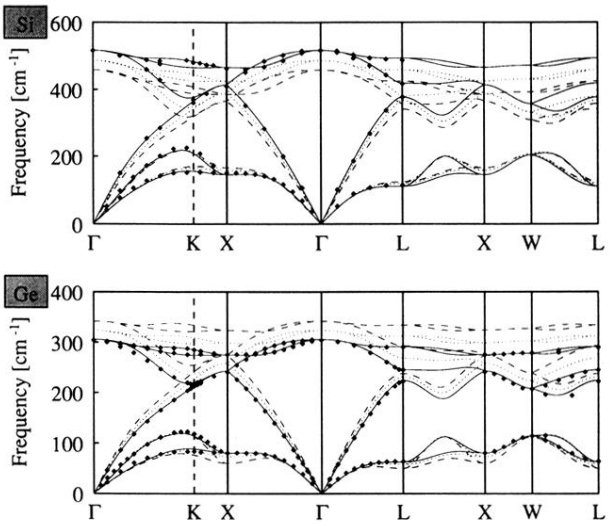

FIG. 1. Calculated phonon dispersions of elemental semiconductors Si and Ge under hydrostatic strain. Solid lines correspond to the unstrained situation, dashed lines correspond to silicon (germanium) at the germanium (silicon) lattice constant. The dotted lines are calculated at the virtual-crystal lattice constant in both cases. Experimental data (diamonds) are from Refs. 20 and 21.

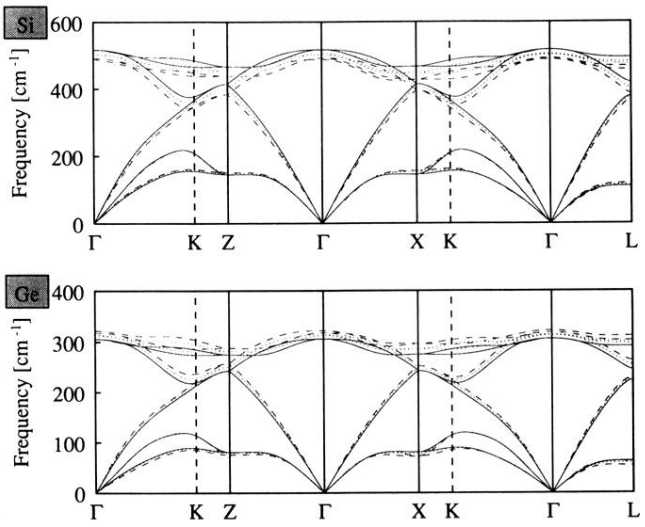

FIG. 2. Calculated phonon dispersions of elemental semiconductors Si and Ge grown on a (001) substrate. Solid lines correspond to the lattice-matched situation, dashed lines correspond to silicon (germanium) grown on a germanium (silicon) substrate. The dotted lines are calculated for a $Si_{0.5}Ge_{0.5}$ substrate in both cases.

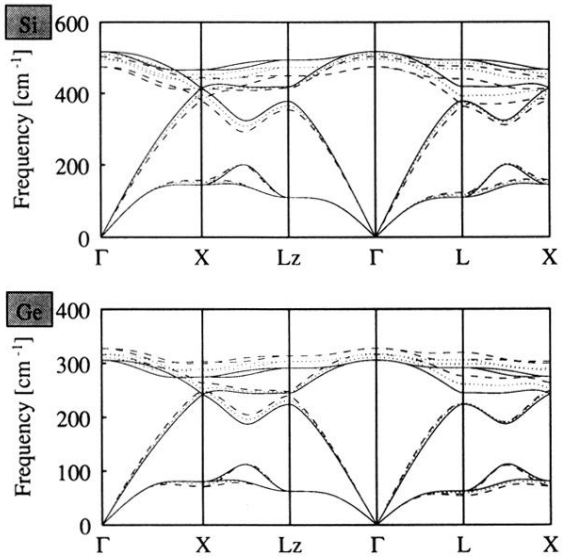

FIG. 3. Calculated phonon dispersions of elemental semiconductors Si and Ge grown on a (111) substrate. Same convention as in Fig. 2.

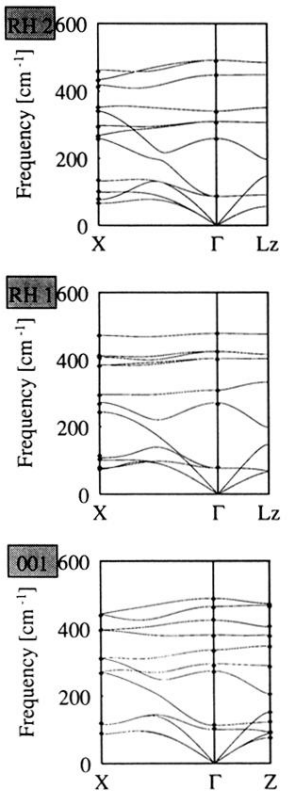

FIG. 4. Calculated phonon dispersions of short-period Si_2/Ge_2 (001) and (111) SL's. In the (111) direction two SL's are possible—RH1 and RH2—depending on the layer stacking. Solid lines are obtained with HIFC's, diamonds show the result of a direct *ab initio* calculation.